Available online at www.sciencedirect.com
ScienceDirect
Journal of Molecular Catalysis A: Chemical 260 (2006) 24–31
JOURNAL OF MOLECULAR CATALYSIS A: CHEMICAL
www.elsevier.com/locate/molcata

Effects of mechanochemical treatment to the vanadium phosphate catalysts derived from $VOPO_4{\cdot}2H_2O$

Y.H. Taufiq-Yap [a,*], C.K. Goh [a], G.J. Hutchings [b], N. Dummer [b], J.K. Bartley [b]

[a] *Department of Chemistry, Universiti Putra Malaysia, 43400 UPM Serdang, Selangor, Malaysia*
[b] *School of Chemistry, Cardiff University, P.O. Box 912, Cardiff CF10 3TB, UK*

Received 18 January 2006; received in revised form 22 May 2006; accepted 27 June 2006
Available online 8 August 2006

Abstract

Modification by using mechanochemical treatment of vanadium phosphate catalysts on the microstructure, morphology, oxygen nature and catalytic performance for *n*-butane oxidation is described and discussed. In this work, the precursor, $VOHPO_4{\cdot}0.5H_2O$ prepared by reduction of $VOPO_4{\cdot}2H_2O$ by isobutyl alcohol was subjected to a high energy planetary ball mill for 30, 60 and 120 min in ethanol. The ball milling process reduced the crystallite size of the catalysts and consequently increased their surface area. The morphologies of the milled catalysts are dependent on milling time. The highest reactivity and mobility of the lattice oxygen species has been achieved by the catalyst milled for 60 min with lower reduction peak temperature and higher amount of oxygen atoms removed. The oxygen species removed from the active V^{4+} phase was shown to be correlated with the rate of reaction. A good relationship was also found between the oxygen species associated with V^{5+} and maleic anhydride selectivity. However, a larger amount of this oxygen species will give a deleterious effect on the conversion rate. The present study demonstrate that the mechanochemical method (with an appropriate duration) effectively enhanced the catalytic activity by increasing the surface area and controlling the reactivity, and that the amount of oxygen species contributed to the partial oxidation of *n*-butane to maleic anhydride.

Keywords: Vanadium phosphate; Mechanochemical; *n*-Butane oxidation; Maleic anhydride

1. Introduction

Vanadium phosphate (VPO) catalysts represent the sole example of an industrial catalyst for the selective oxidation of *n*-butane to maleic anhydride (MA). It is known that the catalytic performance of vanadium phosphates depends on the history of preparation of the catalyst precursor, $VOHPO_4{\cdot}0.5H_2O$ [1,2]. Typically, the active catalyst consists $(VO)_2P_2O_7$ in combination with some V^{5+} phosphate and the topotactically transformation of the precursor to final catalyst [3]. Hence, controlling the physicochemical properties of the precursor is an important factor in determining the physicochemical properties and the performance of the eventual catalyst following activation. In general, V_2O_5 is used as a source of vanadium, and H_3PO_4 is used as a source of phosphorus. Hence, a reducing agent is required to synthesise the V^{4+} precursor phase and a broad range of reducing agents and solvents have been used [4,5]. Initial catalyst preparations [2,4] used water as solvent but most studies, in recent years, have concentrated on the use of alcohols since they can exhibit the dual role of solvent and a reducing agent. Hutchings et al. [6–8] have shown that very active catalysts can be prepared using a two-stage method based on $VOPO_4{\cdot}2H_2O$. In particular, they have found that the alcohol used in the second step to reduce the $VOPO_4{\cdot}2H_2O$ to $VOHPO_4{\cdot}0.5H_2O$ can produce catalyst precursors with better morphology and texture.

Mechanochemical method has been employed in the modification of morphology and texture of the catalyst precursor to improve the catalytic performance of the vanadium phosphate catalyst [9–17]. Zazhigalov et al. [13] reported that the ball milling process could reduce the particle size of catalysts and corresponding increase in the specific surface area. This observation was agreed by Fait et al. [14] who also reported that a decreased particle size and an increased microstrain in the $VOHPO_4{\cdot}0.5H_2O$ precursor would improve the catalytic properties of the V–P–O catalysts. In another report by Hutchings and Higgins [15] on the precursor $VOHPO_4{\cdot}0.5H_2O$ milled in

* Corresponding author. Tel.: +603 8946 6809; fax: +603 8946 6758.
E-mail address: yap@fsas.upm.edu.my (Y.H. Taufiq-Yap).

1381-1169/$ – see front matter © 2006 Elsevier B.V. All rights reserved.
doi:10.1016/j.molcata.2006.06.047

the presence of cyclohexane as solvent and dispersants based on poly-12-hydroxystearic acid, they observed a significant reduction of particle size of the $VOHPO_4{\cdot}0.5H_2O$ (5–0.035 μm) that gave final catalysts with high surface area following activation (>40 $m^2\,g^{-1}$ versus 9 $m^2\,g^{-1}$ without ball milling). They also found that these catalysts are particularly active under fuel rich reaction conditions, when high MA yields can be obtained. Ayub et al. [16] found that Bi-promoted vanadyl pyrophosphate milled in air for relatively short times (5 min) could generate a material that was amorphous in powder X-ray diffraction. They also observed that the blossom secondary morphology of the catalyst was lost under ball milling process. Although they further noted that the ball milling process could increase the specific surface area, the yield and conversion per unit surface area were decreased. Hence, the full benefits that could be expected from the enhanced surface area are unfortunately not produced. Wang et al. [17] showed that the ball milling process broadened the major powder X-ray diffraction peaks, indicating that both a reduction of particle size and a fine variation in local structure could occur in the milled solids, consequently leading to the improvement of catalytic performance of the VPO catalysts.

The purpose of this study is to employ the mechanochemical pretreatment for morphological and textural modification of vanadium phosphate catalysts synthesised via reduction of the $VOPO_4{\cdot}2H_2O$ phase. The structure-activity relationships and the nature and the role of lattice oxygen species of the catalysts are discussed.

2. Experimental

2.1. Catalysts preparation

The $VOPO_4{\cdot}2H_2O$ material was prepared by reacting V_2O_5 (30.0 g from Fluka) with H_3PO_4 (144 cm^3, 85% from Merck) in water (720 cm^3) under reflux with continuous stirring for 24 h. The yellow solid was then recovered by filtration, washed with distilled water (100 cm^3) and followed by acetone (100 cm^3). It was dried at 383 K for overnight. The $VOPO_4{\cdot}2H_2O$ phase was then confirmed by XRD analysis. After that, the synthesised $VOPO_4{\cdot}2H_2O$ (40.0 g) was suspended by rapid stirring into isobutyl alcohol (800 cm^3) and the mixture was refluxed for 21 h with continuous stirring. A blue solid was recovered by filtration and washed with distilled water (100 cm^3) followed by acetone (100 cm^3). The resulting blue solid was further treated in refluxing water (24 ml H_2O/g solid) for 3 h to remove $VO(H_2PO_4)_2$ and was separated by filtration and dried overnight in air at 385 K. Mechanochemical pretreatment of the precursor was carried out by using a high energy planetary ball mill (model Pulverisette 4 from Fritsch) with an agate bowl having 250 ml volume together with fifty 10 mm diameter agate balls. About 18 g of the $VOHPO_4{\cdot}0.5H_2O$ and ethanol as solvent were put together inside the bowl. The bowl spins around its own axis and around a second axis outside its centre at 1400 rpm for 30, 60 and 120 min. The resulting unmilled and milled precursors then undergone calcination in a flow of *n*-butane/air mixture (0.75% *n*-butane in air) for 75 h at 673 K to generate the active catalysts, $(VO)_2P_2O_7$.

2.2. Catalysts characterisation

Brunauer–Emmett–Teller (BET) surface area measurements were carried out by using nitrogen adsorption–desorption at 77 K using a ThermoFinnigan Sorptomatic 1990 instrument.

The bulk chemical composition was determined by using a sequential scanning inductively coupled plasma-atomic emission spectrometer (ICP-AES) Perkin-Elmer Emission Spectrometer Model Plasma 1000.

The average oxidation states of vanadium in all the samples were determined by the method described by Niwa and Murakami [18].

X-ray diffraction (XRD) patterns were obtained using a Shimadzu diffractometer model XRD-6000 employing Cu Kα radiation generated by a Phillips glass diffraction X-ray tube broad focus 2.7 kW type on the catalysts at ambient temperature.

Scanning electron microscopy (SEM) analyses were carried out using a JEOL JSM-6400 electron microscope.

Temperature-programmed reduction (H_2-TPR) in H_2/Ar experiment was performed using a ThermoFinnigan TPDRO 1100 apparatus provided with a thermal conductivity detector. The H_2-TPR analysis of fresh catalysts was done in H_2/Ar stream (5% H_2, 1 bar, 25 $cm^3\,min^{-1}$) with raising the temperature from ambient to 1173 K at 5 K min^{-1}.

2.3. Catalyst testing

The oxidation of *n*-butane to MA was carried out in a fixed-bed microreactor with a standard mass of catalyst (250 mg). The gases *n*-butane and air were fed to the reactor via calibrated mass flow controllers to give a feedstock composition of 1.5% *n*-butane in air. The products were then fed via heated lines to an on-line gas chromatograph for analysis. The reactor comprised of a stainless steel tube with the catalyst held in place by plugs of quartz wool. A thermocouple was located in the centre of the catalyst bed and temperature control was typically ±1 °C. Carbon mass balances of ≥96% were typically observed.

3. Results and discussion

3.1. BET surface area and chemical analysis

Table 1 shows the effect of the ball milling on the ratio of P/V, BET surface area, oxidation state of vanadium as well as percentage of V^{4+} and V^{5+} present in the catalysts. It is found

Table 1
Bulk composition, surface area, average oxidation states and percentage of V^{4+} and V^{5+} oxidation states present in catalysts

Milling time (min)	P/V (ICP)	Surface area ($m^2\,g^{-1}$)	Oxidation state of vanadium		
			V^{4+} (%)	V^{5+} (%)	Average
0	1.00	16	79	21	4.21
30	0.99	19	69	31	4.31
60	0.99	25	84	16	4.16
120	1.00	15	78	22	4.22

that the value of P/V ratios were almost constant, i.e. ∼1.00, indicating that the milling process does not alter the composition of the catalysts. This observation is in agreement with the results obtained by Ji et al. [19]. Furthermore, the bulk ratio of P/V for all catalysts fell in the optimal atomic ratio of P/V in the range of 1.0–1.2 for producing the $(VO)_2P_2O_7$ phase [20].

The surface area for 30 min milled catalysts increased from 16 $m^2\ g^{-1}$ (unmilled) to 19 $m^2\ g^{-1}$ and then further increased to 25 $m^2\ g^{-1}$ after 60 min of milling. The surface area however was drastically reduced to 15 $m^2\ g^{-1}$ for the120 min milled catalyst. Zazhigalov et al. [13] explained that the ball milling process firstly caused repeated fracture of the solid, followed by diminished particle size and a consequent increase in the surface area. Rougier et al. [21] further noted that the fracture of the solid only occurred at a short period of milling process and that longer ball milling process would cause a phenomenon of reagglomeration. The low surface area of 120 min milled material may be due to the agglomeration of unstable particles which are formed by the fracture of the solid.

The average vanadium oxidation number of the material that was milled for 30 min was found higher (4.31) compared to the unmilled counterpart (4.21). This was due to an increment of V^{5+} oxidation state from 21% to 31%. However, the amount of the V^{4+} was increased to 84%, corresponding to a decrease in the average vanadium oxidation state to 4.16 for the catalyst milled for 60 min. Further milling to 120 min slightly decreased the V^{4+} phase to 78% whereas the amount of V^{5+} was increased to 22%.

3.2. X-ray diffraction (XRD)

The XRD patterns of the unmilled and milled precursors, as shown in Fig. 1, gave only the characteristic reflections of vanadyl hydrogen phosphate hemihydrate, $VOHPO_4{\cdot}0.5H_2O$ with the main reflections that appeared at $2\theta = 15.5°$, 19.7°, 24.2°, 27.1°, 28.7°, 30.4°, 37.5° and 49.2° corresponding to

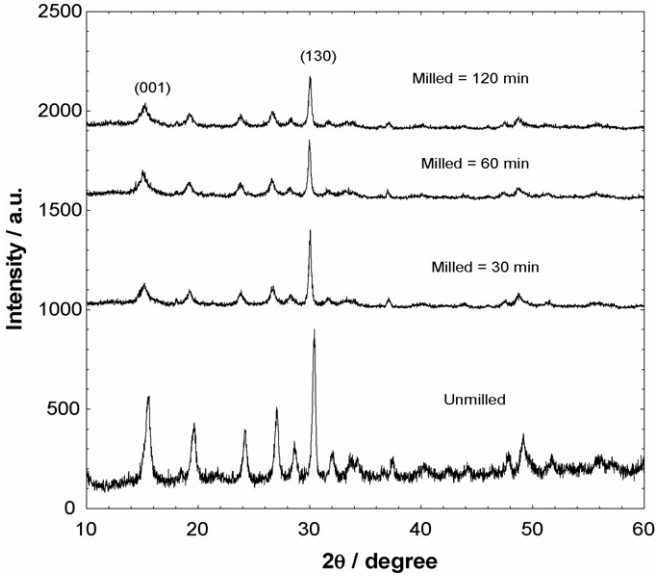

Fig. 1. XRD patterns of unmilled and milled precursors.

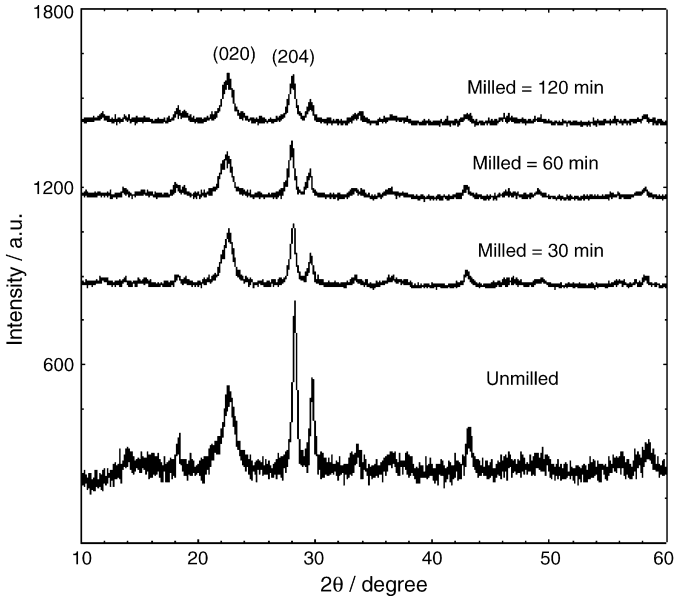

Fig. 2. XRD patterns of unmilled and milled catalysts.

(0 0 1), (1 0 1), (0 2 1), (1 2 1), (2 0 1), (1 3 0), (0 4 0) and (3 3 1) planes, respectively.

The $(VO)_2P_2O_7$ phase (JCPDS File No. 34-1381) shown in Fig. 2 gave main peaks at $2\theta = 22.6°$, 28.2° and 29.7° which correspond to (0 2 0), (2 0 4) and (2 2 1) reflections, respectively. These patterns show that the intensities of the peaks for ball milled catalysts are markedly decreased as compared to the unmilled material. Furthermore, Table 2 indicates that the values of the full width at half maximum (FWHM) were increased, i.e. from 1.16° (unmilled) to 1.26° and 1.37° for the milling time of 30 and 60 min, respectively, along the (0 2 0) plane and from 0.46° (unmilled) to 0.50° and 0.59° for the milling time of 30 and 60 min, respectively, along the (2 0 4) plane. However, further milling to 120 min, the values of FWHM were decreased to 0.37° along the (0 2 0) plane and 0.49° along the (2 0 4) plane. By using the Debye–Scherrer equation, it was found that the crystallite size of the catalysts was reduced with increasing milling duration, i.e. from 7.0 nm (unmilled) to 5.9 nm along the (0 2 0) plane and from 17.8 nm (unmilled) to 13.9 nm along the (2 0 4) plane. The agglomeration occurred in the 120 min milled catalyst; its particle size slightly increased to 6.6 nm along the (0 2 0) plane and 16.7 nm along the (2 0 4) plane and this is in agreement with the evolution of the surface area of samples

Table 2
XRD data of precursors

Milling time (min)	Relative intensity		$I_{(001)}/I_{(130)}$ [a]	FWHM [b] (°)	
	(0 0 1)	(1 3 0)		(0 0 1)	(1 3 0)
0	59	100	0.59	0.48	0.32
30	22	100	0.22	0.26	0.23
60	33	100	0.33	0.30	0.24
120	31	100	0.31	0.24	0.27

[a] Ratios of relative peak intensities.
[b] Full width at half maximum.

upon milling (Table 1). Zazhigalov et al. [13] reported that the reduction of crystallite size, the formation of lattice defects and strain or stress in the bulk of the crystallites, and the increase in amorphous phases in the milled materials are contributed by a decrease in integral intensities of X-ray diffractograms and an increase in FWHM. In addition, increasing milling time also led to an increment in the values of $I_{(0\,2\,0)}/I_{(2\,0\,4)}$, indicating that the exposure of (0 2 0) plane was increased which contained the vanadyl group. Previous literatures [9,22] reported that the best effect in the improvement of catalytic performance can be reached by an increase in the relative exposure of (0 2 0) plane of the $(VO)_2P_2O_7$ because this plane is involved in the reaction of partial oxidation of *n*-butane to MA.

3.3. Scanning electron microscopy (SEM)

The surface morphologies of unmilled and milled catalysts are shown in Fig. 3. The unmilled catalyst (Fig. 3a) is composed of plate-like crystallites, which are arranged into the characteristic rosette-shape clusters. These plate-like structure is related to $(VO)_2P_2O_7$ platelets that preferentially expose the (1 0 0) plane [7]. After milling for 30 and 60 min as shown in Fig. 3b and c, respectively, the catalysts lost their secondary structure of rosette-shape and provide shear forces which allowed the crystal platelets to slide away from one another, thereby exposing more surface plane. This observation may explain the reason for an increase in the surface area after the process of ball milling. However, further milling to 120 min (Fig. 3d) made these crystal platelets broken into smaller pieces thus decreasing the exposure of the surface plane. These smaller platelets are unstable and tendency to agglomerate, causing a decrease in the surface area of the catalyst.

3.4. Temperature-programmed reduction (TPR) in H_2/Ar

In order to investigate the effect of ball milling on the redox properties, amount and nature of the oxygen species of the catalysts, H_2-TPR experiments were performed on the unmilled and milled catalysts. Fig. 4 shows the profiles of H_2-TPR, and total amount of oxygen removed and the values of reduction activation energies are shown in Table 3.

The unmilled catalyst gave characteristic two reduction peaks at the region of 400–1100 K. These peaks occurred at 779 and 990 K, where the first peak is the reduction of V^{5+} phase whereas the second peak is assigned to the removal of lattice oxygen from the active V^{4+} phase [23]. The amount of oxygen removed from both peaks is 3.85×10^{20} and 1.20×10^{21} atom g^{-1}, respectively, with an oxygen ratio for V^{5+} to V^{4+} of 0.32. The milled catalysts show similar reduction profiles to the unmilled material. It was found that the 30 min milled catalyst slightly increased the temperature of the first peak with 20 K of increment, but that of the second peak decreased by 14 K. Nevertheless, 60 min milled catalyst also showed shifts of both reduction peaks to lower temperatures, i.e. 760 and 953 K. How-

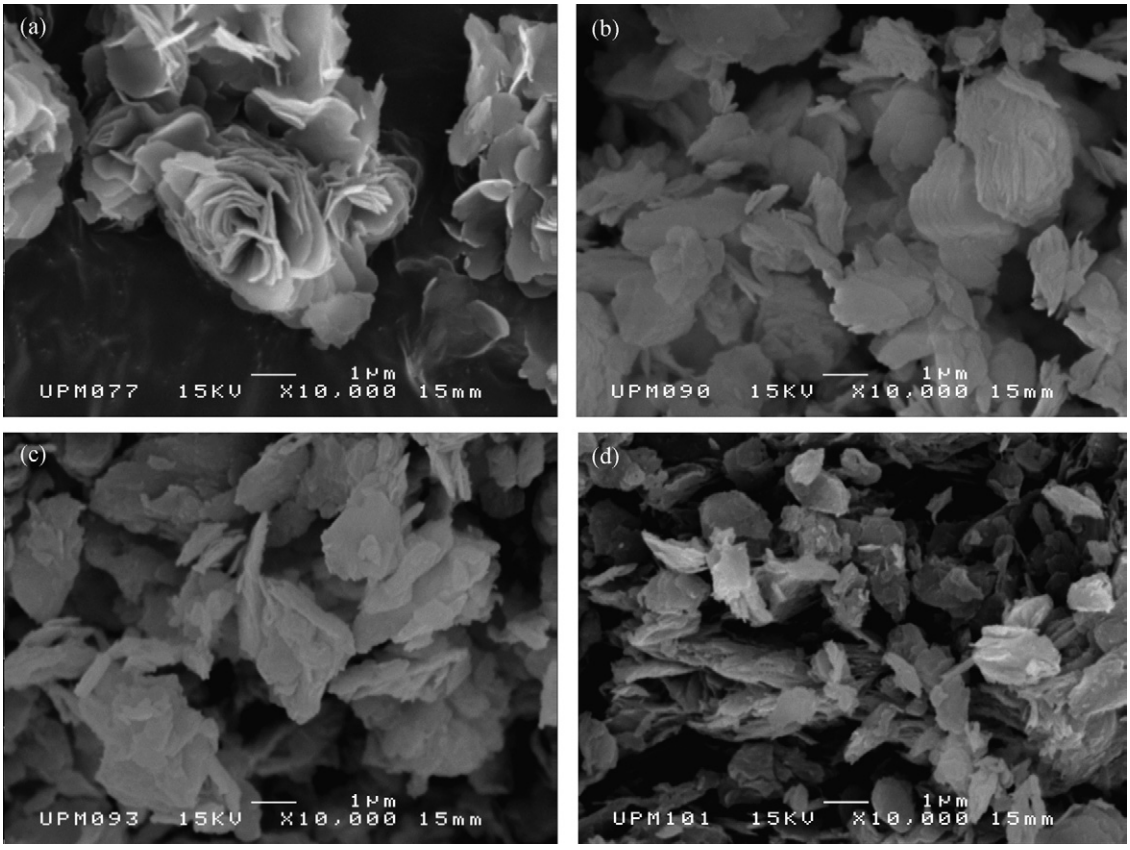

Fig. 3. SEM micrographs of (a) unmilled, (b) milled = 30 min, (c) milled = 60 min and (d) milled = 120 min.

Table 3
XRD data of catalysts

Milling time (min)	Relative intensity		$I_{(020)}/I_{(204)}$[a]	FWHM[b] (°)		Crystallite size[c] (nm)	
	(020)	(204)		(020)	(204)	(020)	(204)
0	48	100	0.48	1.16	0.46	7.0	17.8
30	83	100	0.83	1.26	0.50	6.4	16.5
60	89	100	0.89	1.37	0.59	5.9	13.9
120	100	98	1.01	0.37	0.49	6.6	16.7

[a] Ratios of relative peak intensities.
[b] Full width at half maximum.
[c] Crystallite size was calculated accordingly to Debye–Schrrer equation.

ever, a further milling to 120 min shifted the first reduction peak to higher temperature, i.e. 789 K, but the second reduction peak appeared at lower temperature, i.e. 960 K as compared to unmilled catalyst. The amount of oxygen species released associated with V^{5+} significantly increased to 5.69×10^{20} atom g^{-1} for 30 min milled catalyst. However, further milling to 60 min reduced the amount to 3.29×10^{20} atom g^{-1}. The catalyst subjected to mechanochemical pretreatment for 120 min showed almost identical amount of oxygen removed related to V^{5+}, i.e. 3.81×10^{20} atom g^{-1} as compared to unmilled material. The amount for oxygen species removed from the second reduction peak, which is attributed to the reduction of V^{4+} decreased to (9.35 and 9.81) $\times 10^{20}$ atom g^{-1} for milling time of 30 and 120 min, respectively. Interestingly for 60 min milled catalyst, the amount of oxygen significantly increased to 1.43×10^{21} atom g^{-1} with an increment of 19.2%. The oxygen atom released ratio of V^{5+} to V^{4+} for milled catalysts is 0.61, 0.23 and 0.39 for milling time of 30, 60 and 120 min, respectively. The results show that 60 min of milling in ethanol is the optimum duration to obtain a highly active catalyst as this catalyst possesses highest amount of active V^{4+}–O^{-} pair for *n*-butane activation and an appropriate oxygen species ratio associated with V^{5+} to V^{4+}.

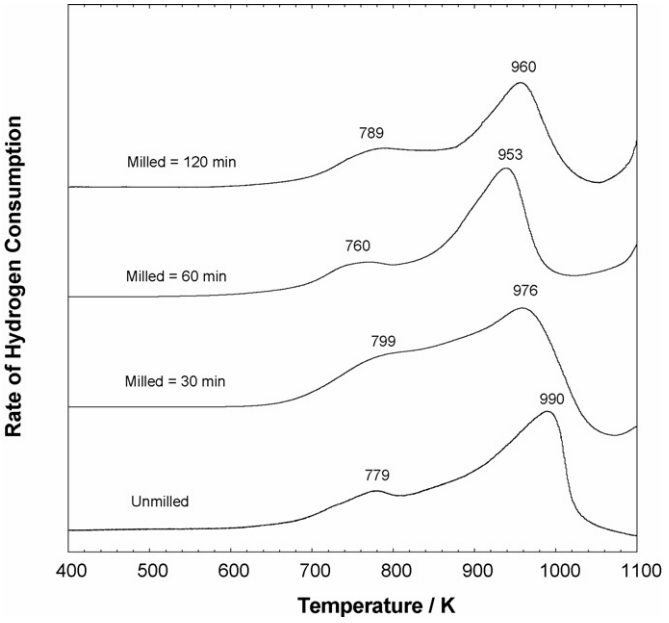

Fig. 4. H_2-TPR profiles of unmilled and milled catalysts.

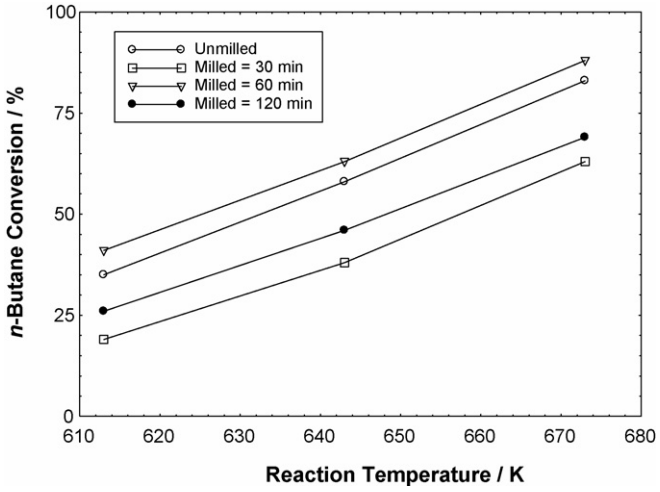

Fig. 5. *n*-Butane conversion as a function of the reaction temperatures.

3.5. Catalytic evaluation

Fig. 5 shows *n*-butane conversion as a function of the reaction temperatures, whereas the selectivity to MA is plotted against the reaction temperature in the range of 613–673 K is given in Fig. 6. All catalysts exhibited an increase in *n*-butane conversion with increasing temperature, and a reduction of MA selectivity when the temperature increased. The 60 min milled catalyst

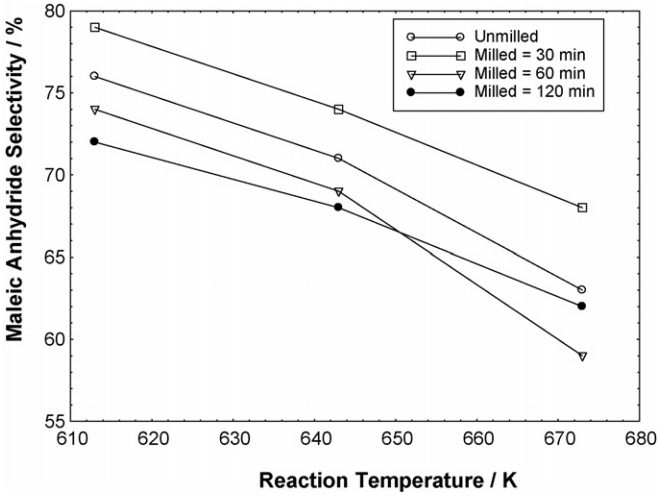

Fig. 6. MA selectivity as a function of the reaction temperatures.

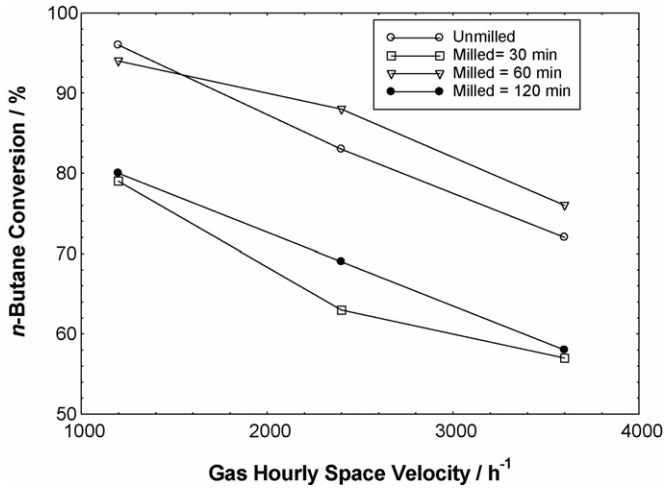

Fig. 7. *n*-Butane conversion as a function of the gas hourly space velocity.

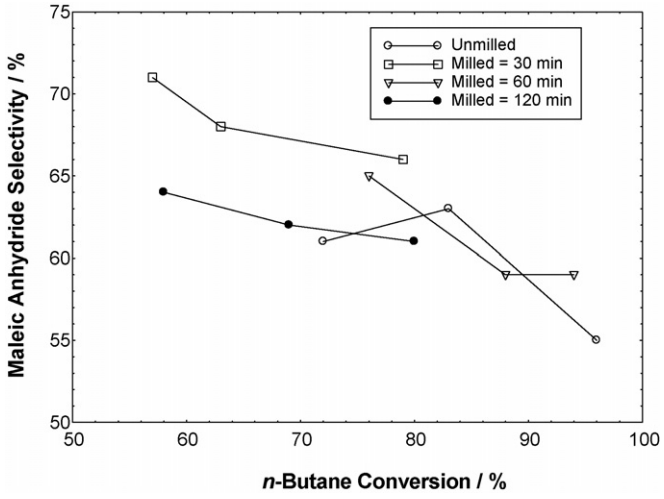

Fig. 9. MA selectivity as a function of the *n*-butane conversion ($T = 673$ K).

was found to be the most active in the whole range of reaction temperatures tested as compared to others. With respect to the *n*-butane conversion and MA selectivity as a function of the gas hourly space velocity (GHSV) as shown in Figs. 7 and 8, respectively, the 60 min milled catalyst also appeared the most active. The 30 min milled catalyst was found to give the highest MA selectivity as shown in Fig. 9.

Table 4 summarises the catalytic performance of unmilled and milled catalysts at reaction temperature of 673 K and GHSV of 2400 h^{-1}. The results show that the mechanochemical pretreatment employed in the preparation of the catalysts had an impact on the catalytic performance, especially the conversion of *n*-butane. For the catalyst milled for 30 min, surprisingly it drastically decreases the conversion of *n*-butane from 83% (unmilled) to 63%. However, a further milling to 60 min caused an increase in the conversion to 88%, which is an optimal value milling duration since the conversion was shown significantly decreased when milling was extended to 120 min, i.e. 69%. On the other hand, the MA selectivity of 30 min milled catalyst was found to be increased from 63% (unmilled) to 68%. A longer milling duration reduced the MA selectivity to 59% and 60% for 60 and 120 min milled catalysts, respectively. Nevertheless, all milled samples gave lower intrinsic activity compared to the unmilled catalyst (Table 5).

Although the 30 min milled catalyst produced slightly higher surface area than the unmilled material, but it exhibited significantly low *n*-butane conversion. Nevertheless, it showed an improvement in the formation of valuable product because it produced higher MA and less CO and CO_2 as compared to those without and longer times of milling. This may due to an increase in the amount of lattice oxygen species removed associated with the V^{5+} phase as shown in H_2-TPR analysis. The V^{5+} sites was not detectable by XRD analysis which may be isolated on the surface of $(VO)_2P_2O_7$ phase [24]. In the plot of the relationship of *n*-butane conversion and MA selectivity to oxygen species associated with V^{5+} phase as shown in Figs. 10 and 11, a good correlation of the oxygen species associated with V^{5+} and MA

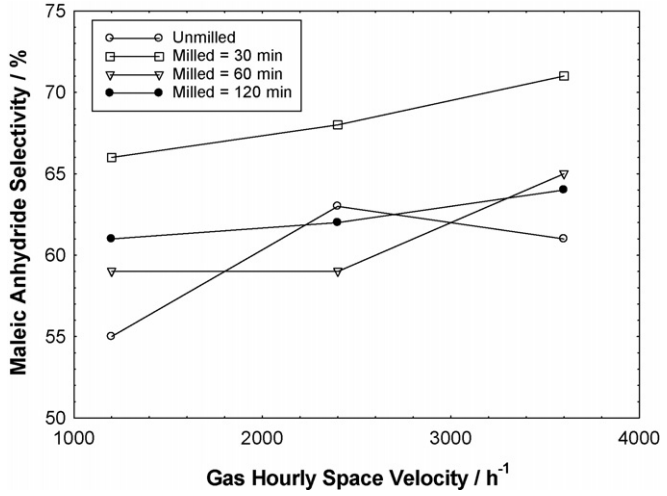

Fig. 8. MA selectivity as a function of the gas hourly space velocity.

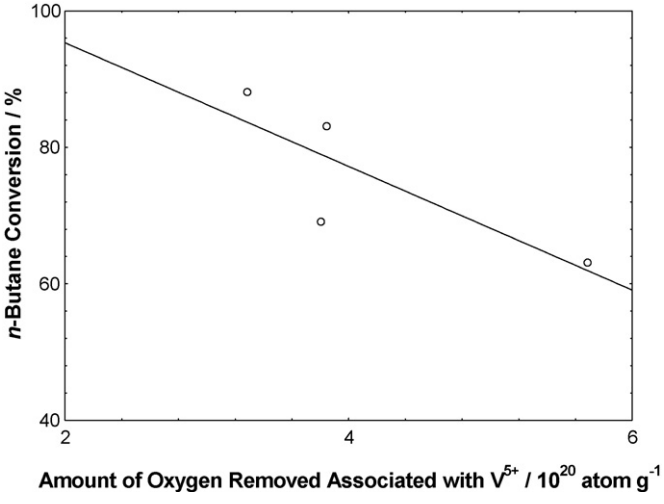

Fig. 10. *n*-Butane conversion as a function of amount of oxygen removed associated with V^{5+}.

Table 4
Total amount of oxygen atoms removed, values of reduction activation energies and ratio for oxygen removal of V^{5+}/V^{4+} by reduction in H_2/Ar for unmilled and milled catalysts

Milling time (min)	Peak	T_{max} (K)	Reduction activation energy, E_r (kJ mol^{-1})	Total amount of oxygen removed (mol g^{-1})	Total amount of oxygen removed (atom g^{-1})	Ratio for oxygen removal of V^{5+}/V^{4+}
	1	779	130.3	6.39×10^{-4}	3.85×10^{20}	
0	2	990	165.5	2.00×10^{-3}	1.20×10^{21}	
	Total			2.64×10^{-3}	1.59×10^{21}	0.32
	1	799	133.6	9.45×10^{-4}	5.69×10^{20}	
30	2	976	163.2	1.55×10^{-3}	9.35×10^{20}	
	Total			2.50×10^{-3}	1.50×10^{21}	0.61
	1	760	127.1	5.47×10^{-4}	3.29×10^{20}	
60	2	953	159.4	2.38×10^{-3}	1.43×10^{21}	
	Total			2.93×10^{-3}	1.76×10^{21}	0.23
	1	789	131.9	6.33×10^{-4}	3.81×10^{20}	
120	2	960	160.5	1.63×10^{-3}	9.81×10^{20}	
	Total			2.26×10^{-3}	1.36×10^{21}	0.39

selectivity was observed. However, a large amount of this oxygen species would also reduce the conversion of *n*-butane. Earlier researchers [3,25–28] reported the important of the lattice oxygen associated with V^{5+} in determining the selectivity to MA. Coulston et al. [29] reported that by using time-resolved X-ray absorption spectroscopy, V^{5+} species are kinetically significant for the production of MA. Thus, there is considerable evidence that V^{5+} sites are a requirement if the catalyst is to simultaneously exhibit good activity and selectivity.

High *n*-butane conversion obtained for the 60 min milled catalyst can be related to the reducibility of the catalysts because this reaction involved a redox mechanism [30]. The lattice oxygen of this catalyst was found to be more reducible, reactive and mobile. It exhibited lower reduction peak temperature accompanied by higher amount of oxygen species removed associated with V^{4+} phase which was suggested as the centre for of *n*-butane activation [28,31]. The *n*-butane conversion is plotted (Fig. 12) versus the amount of oxygen removed associated with V^{4+} phase for this four catalysts, which presents a direct correlation between them. This result confirmed that this oxygen species assigned to O^- contributed to the activity of the catalyst. Due to the p-type semi-conductive character of vanadium phosphate catalyst, it was proposed that charge carrier is p^+ holes known as strong oxidizing agents. They correspond to O^- species in the solid which would result from a charge transfer equilibrium creating V^{4+}–O^- ion pairs. Such a reactive pair associating with a coordinative unsaturated V^{4+} and O^- species should explain the initial *n*-butane activation with H-abstraction by O^- species to form MA [31]. A good correlation was also shown between the percentages of V^{4+} obtained by redox titration with the *n*-butane conversion (Fig. 13). A longer milling duration to 120 min gave a poorer performance which was explained by a lower surface area and higher ratio of oxygen species removed from V^{5+} to V^{4+} phases which was obtained from H_2-TPR analysis. A lower amount of active oxygen species, O^-, which is related to V^{4+}, also contributed to the poor activity.

Table 5
Catalysts performance of unmilled and milled vanadium phosphate for the oxidation of *n*-butane[a]

Milling time (min)	*n*-Butane conversion (%)	Product selectivity (%)			Intrinsic activity[b] ($\times 10^{-5}$ mol MA m^{-2} h^{-1})
		MA	CO	CO_2	
0	83	63	18	19	4.18
30	63	68	15	17	2.96
60	88	59	19	22	2.71
120	69	62	17	21	3.69

[a] Reaction conditions: 673 K, 1.5% *n*-butane in air, GHSV = 2400 h^{-1}.
[b] Intrinsic activity: mol maleic anhydride (MA) formed m^{-2} catalyst h^{-1}.

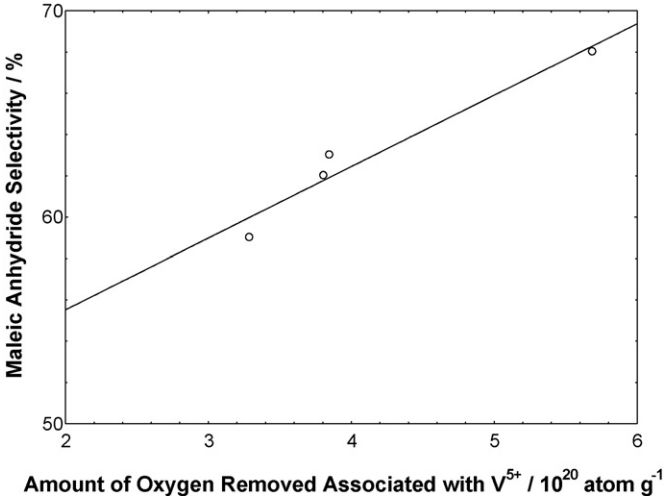

Fig. 11. MA selectivity as a function of amount of oxygen removed associated with V^{5+}.

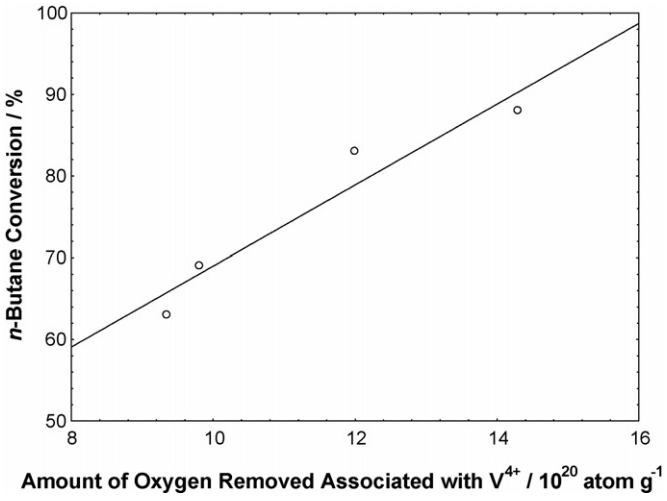

Fig. 12. *n*-Butane conversion as a function of amount of oxygen removed associated with V^{4+}.

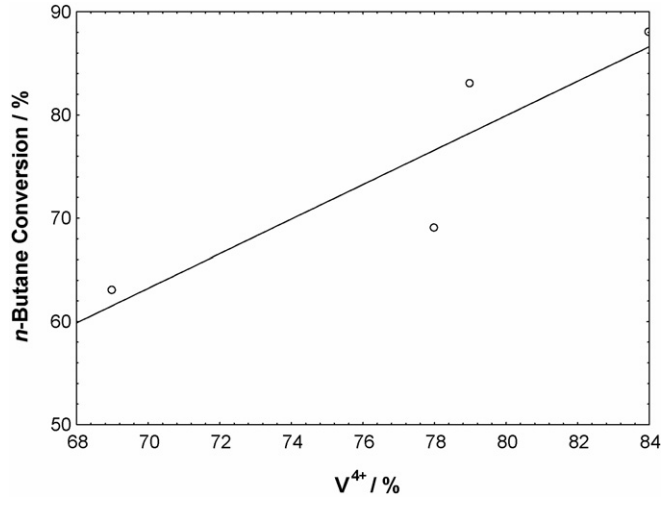

Fig. 13. *n*-Butane conversion as a function of V^{4+}.

4. Conclusions

The adoption of mechanochemical pretreatment on a catalyst precursor in this study increased the full width at half maximum (FWHM) and reduced the crystallite size of the catalysts and consequently increased their surface area without affecting the principal phase structures of $VOHPO_4{\cdot}0.5H_2O$ and $(VO)_2P_2O_7$ as well as the P/V ratios. The increase in the surface area may be associated with the morphologies of the catalysts which prevent the crystal platelets from tightly stacking together, thereby exposing more surface plane. However, an extension of milling time to 120 min led to a decrease in the surface area of the catalyst which due to the agglomeration of the unstable fractured solids. The 30 min milled catalyst was found to increase the average vanadium oxidation number of the catalyst from 4.21 (unmilled) to 4.31. However, further milling to 60 and 120 min reduced the number to 4.16 and 4.22, respectively. The oxygen species of 60 min milled catalyst was found to be the most reactive with high amount of oxygen species (O^-) associated with the active V^{4+} phase. A good direct relationship was established between the reaction rate and the oxygen species associated with V^{4+}. Thus, the dependence of the *n*-butane activity on the very reactive oxygen species suggested that the release of O^- anion from the surface of $(VO)_2P_2O_7$ is the rate determining step for the oxidation of *n*-butane.

Acknowledgement

Financial assistance from Malaysian Ministry of Science, Technology and Innovation is gratefully acknowledged.

References

[1] G.J. Hutchings, Appl. Catal. 72 (1991) 1.
[2] G.J. Hutchings, J. Mater. Chem. 14 (2004) 3385.
[3] G. Centi, F. Trifiro, J.R. Ebner, V.M. Franchetti, Chem. Rev. 88 (1988) 55.
[4] B.K. Hodnett, Catal. Rev. Sci. Eng. 27 (1985) 373.
[5] J.W. Johnson, D.C. Johnston, A.J. Jacobson, J.F. Brody, J. Am. Chem. Soc. 106 (1984) 8123.
[6] G.J. Hutchings, R. Olier, M.T. Sananes, J.C. Volta, in: V.C. Corberán, S.V. Bellón (Eds.), New Developments in Selective Oxidation II, Elsevier, Amsterdam, 1994.
[7] C.J. Kiely, S. Sajip, I.J. Ellison, M.T. Sananes, G.J. Hutchings, J.C. Volta, Catal. Lett. 33 (1995) 357.
[8] G.J. Hutchings, M.T. Sananes, S. Sajip, C.J. Kiely, A. Burrows, I.J. Ellison, J.C. Volta, Catal. Today 33 (1997) 161.
[9] V.A. Zazhigalov, J. Haber, J. Stoch, L.V. Bogutskaya, I.V. Bacherikova, Appl. Catal. A: Gen. 135 (1996) 155.
[10] A.S. Horowita, C.M. Blackstone, A.W. Sleight, G. Teufer, Appl. Catal. 38 (1988) 193.
[11] K. Shima, M. Ito, M. Murayama, M. Hatano, Stud. Surf. Sci. Catal. 92 (1995) 355.
[12] K. Inumaru, T. Okuhara, M. Misono, Chem. Lett. (1992) 1955.
[13] V.A. Zazhigalov, J. Haber, J. Stoch, A. Kharlamov, L.V. Bogutskaya, I.V. Bacherikova, A. Kowal, Solid State Ionics 101–103 (1997) 1257.
[14] M. Fait, B. Kubias, H.-J. Eberle, M. Estenfelder, U. Steinike, M. Schneider, Catal. Lett. 68 (2000) 13.
[15] G.J. Hutchings, R. Higgins, Appl. Catal. A: Gen. 154 (1997) 103.
[16] I. Ayub, D.S. Su, M. Willinger, A. Kharlamov, L. Ushkalov, V.A. Zazhigalov, N. Kirillova, R. Schlögl, Phys. Chem. Chem. Phys. 5 (2003) 970.
[17] X. Wang, L. Xu, X. Chen, W. Ji, Q. Yan, Y. Chen, J. Mol. Catal. A: Chem. 206 (2003) 261.
[18] M. Niwa, Y. Murakami, J. Catal. 76 (1982) 9.
[19] W. Ji, L. Xu, X. Wang, Z. Hu, Q. Yan, X. Chen, Catal. Today 74 (2002) 101.
[20] G. Centi, Catal. Today 16 (1993) 5.
[21] A. Rougier, S. Soiron, I. Haihal, L. Aymard, B. Taouk, J.-M. Tarascon, Powder Technol. 128 (2002) 139.
[22] J. Haber, V.A. Zazhigalov, J. Stoch, L.V. Bogutskaya, I.V. Bacherikova, Catal. Today 33 (1997) 39.
[23] B.T. Pierini, E.A. Lombardo, Mater. Chem. Phys. 92 (2005) 197.
[24] J.C. Volta, Top. Catal. 15 (2001) 121.
[25] M.L. Granados, J.C. Conesa, M. Fernandez-Garcia, J. Catal. 141 (1993) 671.
[26] M.T. Sananes, A. Tuel, G.J. Hutchings, J.C. Volta, J. Catal. 166 (1997) 388.
[27] J.C. Volta, C.R. Acad. Sci. Paris, Série IIc: Chim./Chem. 3 (2000) 717.
[28] E. Bordes, Catal. Today 16 (1993) 61.
[29] G.W. Coulston, S.R. Bare, H. Kung, K. Birkeland, G.K. Bethke, R. Harlow, H.N., P.L. Lee, Science 275 (1997) 191.
[30] G. Centi, F. Cavani, F. Trifiro, Selective Oxidation by Heterogeneous Catalysis, Kluwer Academic/Plenum, New York, 2001.
[31] J.-M. Herrmann, P. Vernoux, K.E. Béré, M. Abon, J. Catal. 167 (1997) 106.